Growth of dandelion-shaped CuInSe2 nanostructures by a two-step solvothermal process

Zhou, Wenwen; Yin, Zongyou; Sim, Daohao; Zhang, Hua; Ma, Jan; Hng, Huey Hoon; Yan, Qingyu

2011

Zhou, W., Yin, Z., Sim, D., Zhang, H., Ma, J., Hng, H. H., & Yan, Q. (2011). Growth of dandelion-shaped CuInSe2 nanostructures by a two-step solvothermal process. Nanotechnology, 22, 195607.

https://hdl.handle.net/10356/95684

https://doi.org/10.1088/0957-4484/22/19/195607

Growth of dandelion-shaped $CuInSe_2$ nanostructures by a two-step solvothermal process

Wenwen Zhou, Zongyou Yin, Dao Hao Sim, Hua Zhang, Jan Ma, Huey Hoon Hng and Qingyu Yan[1]

School of Materials Science and Engineering, Nanyang Technological University, 50 Nanyang Avenue, Singapore 639798, Singapore

E-mail: alexyan@ntu.edu.sg

[1] *Author to whom any correspondence should be addressed.*

ABSTRACT

$CuInSe_2$ (CIS) nanodandelion structures were synthesized by a two-step solvothermal approach. First, InSe nanodandelions were prepared by reacting $In(acac)_3$ with trioctylphosphine-selenide (TOP-Se) in 1-octadecene (ODE) at 170 ◦C in the presence of oleic acid. These InSe dandelions were composed of polycrystalline nanosheets with thickness <10 nm. The size of the InSe dandelions could be tuned within the range of 300 nm^{-2} μm by adjusting the amount of oleic acid added during the synthesis. The InSe dandelion structures were then reacted with $Cu(acac)_2$ in the second-step solvothermal process in ODE to form CIS nanodandelions. The band gap of the CIS dandelions was determined from ultraviolet (UV) absorption measurements to be ∼1.36 eV, and this value did not show any obvious change upon varying the size of the CIS dandelions. Brunauer–Emmett–Teller (BET) measurements showed that the specific surface area of these CIS dandelion structures was 44.80 $m^2\ g^{-1}$, which was more than five times higher than that of the CIS quantum dots (e.g. 8.22 $m^2\ g^{-1}$) prepared by using reported protocols. A fast photoresponsive behavior was demonstrated in a photoswitching device using the 200 nm CIS dandelions as the active materials, which suggested their possible application in optoelectronic devices.

S Online supplementary data available from stacks.iop.org/Nano/22/195607/mmedia (Some figures in this article are in colour only in the electronic version)

1. INTRODUCTION

Copper indium diselenide (CIS) based chalcopyrite compounds [1] are attractive candidates for the construction of low-cost-per-watt solar cells due to their high optical absorption coefficient [2, 3] and the suitable width of their absorption band gap (0.8–1.1 eV), which matches the red edge of the solar spectrum [4–6]. Thin film solar cells made of CIS based chalcopyrites are able to achieve conversion efficiencies as high as 21.5% [7]. Recently, the synthesis of CIS nanostructures [8–11] has attracted great interest due to the flexibility of the processes, easily controllable stoichiometry, size and shape, which may simplify the solar device fabrication, e.g. by ink-printing [9], as compared to thin film processes. Various processes have been developed to grow CIS nanocrystals with

controllable morphology and phases, e.g. solvothermal growth of nanorings [10], nanorods [12, 13], nanoparticles [9, 11, 14–17], and nanowires [18]; vapor– liquid–solid growth of nanowires [19]; solid-state-reaction growth of nanowires [20]. These synthesis processes may be considered as attractive bottom-up approaches for solar device fabrication. Usually, CIS synthesized using the solvothermal method forms p-type materials, which are promising for good performance in conventional solar cell fabrication. On the other hand, hierarchical structures of nanocrystals, e.g. assembly of nanoribbons into dandelion shapes [21], combines the features of micrometer-(highly stable) and nanometer-scaled (highly activated) building blocks [21–27]. Although several processes have been developed to produce hierarchical-structured inorganic materials such as metal oxide [21, 26], metal hydrate [27], sulfide [25], or metal alloy [28, 29], there are no reports on the synthesis of a CIS hierarchical structure, which could be an interesting solar cell active material with high surface area.

Herein, we report a facile synthesis of a dandelion-shaped $CuInSe_2$ nanostructure by a two-step solvothermal process. First, dandelion-shaped InSe composed of nanosheets was prepared by injecting trioctylphosphine-selenide (TOP-Se) solution into $In(acac)_3$ dissolved in 1-octadecene (ODE) at 170 ◦C in the presence of oleic acid. The size of the dandelion structures could be tuned by adjusting the amount of oleic acid added. These InSe dandelions were then used to react with $Cu(acac)_2$ in ODE at 120 ◦C to form CIS with the dandelion shape retained. The Brunauer–Emmett–Teller (BET) measurements showed that the specific surface area of these CIS dandelion structures was 44.80 $m^2\ g^{-1}$, which was more than five times higher than that of CIS quantum dots prepared using the reported protocols [8, 9], e.g. 8.22 $m^2\ g^{-1}$. These CIS dandelions showed interesting photo-sensitivities when tested as photoswitches. The 200 nm CIS dandelions were used as the active materials in the photoswitching device, and a fast photoresponsive behavior was observed.

2. EXPERIMENTAL SECTION

2.1. Synthesis of InSe.

The trioctylphosphine-selenide solution (1 M, TOP-Se) was prepared in advance by dissolving 789.6 mg of selenium powder in 10 ml of TOP with moderate stirring. In a typical synthesis, 103 mg (0.25 mmol) indium (III) acetylacetonate, 0.25 ml oleic acid, and 5 ml 1-octadecene (ODE) were added into a 100 ml three-neck round flask. The solution was stirred at 150◦C under argon flow for 30 min. After dissolving, the temperature of the mixture was increased to 170 ◦C and 0.8 ml of 1 M TOP-Se solution was rapidly injected into the flask. The solution was refluxed at 170◦C for 10 min and then cooled down to room temperature in ambient. The dark-red-colored precipitates were cleaned by repeated washing with hexane and centrifuging several times. The InSe precipitates were then used in the second-step synthesis of $CuInSe_2$.

2.2. Synthesis of $CuInSe_2$.

25 mg copper (II) acetylacetonate, 50 mg dodecanediol, 100 μl dodecanthiol, and 10 ml ODE were loaded into a three-neck flask and heated up to 120◦C under argon flow. The InSe obtained in the first synthesis process was then dispersed in ODE and was quickly injected into the flask and refluxed at 120◦C for 1 min. The color of the precipitates changed from dark red to black during the second synthesis step. The precipitates were collected and purified by washing with hexane and centrifuging. The samples were annealed under Ar atmosphere at 350◦C to improve the crystallinity and to remove the surface capping ligands to increase their electrical conductivity for photo-sensitivity testing.

2.3. Characterization of samples

The as-prepared samples were characterized via x-ray diffraction (XRD) in a Bruker D8 Advance diffractometer with a Cu Kα radiation source. Scanning electron microscopy (SEM) and energy-dispersive x-ray analysis (EDS) were carried out with a FESEM (JEOL JSM7600). Transmission electron microscopy (TEM) images and high resolution TEM images were taken with a JEOL JSM-2100F operating at 200 kV. Absorption spectra were recorded with a Perkin Elmer ultraviolet–visible–near infrared (UV–vis–NIR) Lambda 900 spectrophotometer. The surface area of the products was measured by the BET method using nitrogen adsorption and desorption isotherms on a Micrometrics ASAP2020 system.

The photoswitching device was fabricated with reduced graphene oxide (rGO) as the electrode [30] and the performance was measured by the electrochemical workstation (CHI 600C, CH Instrument Inc., USA). The reduced graphene oxide (rGO) electrode (∼10 nm) on SiO_2(300 nm)/Si substrate was prepared based on the reported method [31]. The 200 nm CIS dandelions were dispersed in ethanol and sprayed onto the rGO/SiO_2/Si substrates to form 2 μm thick films, followed by annealing under Ar atmosphere at 350◦C for 30 min. The photocurrent of the CIS dandelion film was measured in a three-electrode electrochemical cell with a standard saturated Ag/AgCl and a Pt wire as the reference and counter electrodes, respectively. The electrolyte used for this photocurrent experiment was 0.5 M Na_2SO_4. The illumination source for the photocurrent generation was from a 150 W halogen lamp with its ON and OFF states manually controlled. The whole measurement was conducted at room temperature in open air.

3. RESULTS AND DISCUSSION

The first-step reaction of the synthesis was carried out by reacting $In(acac)_3$ with TOP-Se in ODE in the presence of oleic acid. The XRD pattern (see figure 1) of the products revealed that all the diffraction peaks were indexed to the rhombohedral InSe phase (JCPDS Card No. 42–0919). The representative SEM and TEM images of the InSe are displayed in figure 2, which showed the dandelion-shaped nanostructures. Varying the molar ratio between oleic acid and indium acetylacetonate, $I_{oleic/In}$, led to the changing of the size of these InSe dandelions, e.g. decreasing $I_{oleic/In}$ from 12 to 3 resulted in a

decrease in the average size of the dandelions from 1.5 μm to 300 nm (see figures 2(a) and (b). The particles were mono-distributed with polydispersity index less than 15% (see supporting information S1 stacks.iop.org/ Nano/22/195607/mmedia). This was mainly attributed to the high concentration of oleic acid that led to a slower nucleation and growth process, which resulted in the formation of larger structures [32–36]. The size of the dandelions terminated at ∼2 μm when more oleic acid was added during synthesis. The higher temperature (e.g. 220 ◦C) led to faster reaction and merged the separate dandelions. The TEM images (see figures 2(c) and (d)) showed that the dandelion structures were composed of nanosheets with a thickness of <5 nm. The nanosheets were folded together into spheres to minimize the total surface energy. The high resolution (HR) TEM image (see figure 2(d)) indicated that the InSe nanosheets in the dandelion structures were polycrystalline with preferred exposure of (001) facets, which was revealed by the spot pattern observed in the selected area electron diffraction (SAED) pattern obtained from the InSe nanosheet (see inset in figure 1(d)). During our experiments, we found that the presence of oleic acid was important to confine the growth of the InSe dandelions, possibly due to their preferred attachment on the (001) planes of InSe. Without using oleic acid during the synthesis, the samples obtained were agglomerated clusters without defined morphology (see supporting information figures S2a and b stacks.iop.org/Nano/ 22/195607/mmedia).

The as-prepared InSe dandelions were reacted with $Cu(acac)_2$ in ODE at 120 °C in order to form $CuInSe_2$. The XRD pattern (see figure 3) of the as-prepared samples from the second-step reaction showed diffraction peaks corresponding to the chalcopyrite $CuInSe_2$ phase (JCPDS 23-0209). A systematic peak-position shift was observed, which was probably due to the residual stress in the crystal lattice created during the formation of CIS. The proposed chemical reactions that occurred are listed as follows:

$$InSe + Cu^{2+} \rightarrow In^{2+} + CuSe \quad (1)$$
$$CuSe + InSe \rightarrow CuInSe_2. \quad (2)$$

The replacement reactions between In^{2+} and Cu^{2+} could create plenty of defects and disorder, which possibly caused the shift in the peak position as revealed by the XRD pattern of the as-prepared CIS dandelions. Annealing the samples at 350 °C under Ar atmosphere led to re-crystallization, which might have released the residual stress by improving the long-range ordering of the lattice. The peaks of the annealed sample matched well with the $CuInSe_2$ (JCPDS 23-0209) without any obvious peak shift.

The SEM and TEM images (see figures 4(a) and (b)) revealed that the as-prepared $CuInSe_2$ from the second-step reaction was still dandelion-shaped. The size of the resulting $CuInSe_2$ was close to that of the InSe dandelions initially added during this second-step reaction. The EDX analysis (see supporting information figure S3 stacks.iop.org/Nano/22/ 195607/mmedia) carried out in the TEM showed that the atomic ratio of the $CuInSe_2$ was Cu:In:Se = 28:27:45. The HRTEM observations (see figure 4(c)) indicated that the grain size of the as-prepared CIS was 5–10 nm. This observation agreed well with the average grain size estimated from the peak width of the corresponding XRD pattern (see figure 3) using Scherrer's equation. Annealing the as-

prepared $CuInSe_2$ at 350 ◦C for 30 min did not cause much alteration to the morphology of the dandelions (see figures 4(d) and (e)). The HRTEM image (see figure 4(f)) displayed the lattice fringes with a spacing of 0.34 nm that matched well with the interplanar spacing of the {112} planes of the chalcopyrite $CuInSe_2$.The grain size of the annealed $CuInSe_2$ increased to ∼10 nm as estimated from the peak width of the corresponding XRD pattern (see figure 3). During the second-step reaction, it was found that the addition of extra Cu precursors led to the formation of metallic Cu in the annealed samples, as shown from the XRD results (see supporting information figure S4 stacks.iop.org/Nano/22/195607/mmedia).

The UV absorption spectra obtained for both the as-prepared InSe and annealed CIS dandelions are shown in figure 5. It was found that the size of InSe and $CuInSe_2$ dandelions did not have obvious effects on their UV absorption spectra. For the 200 nm InSe dandelions, the absorption spectrum exhibited a threshold at ∼737 nm (e.g. ∼1.68 eV), which corresponded to the expected band gap in the range of ∼1.3–1.7 eV for bulk indium selenide [37, 38]. The absorption spectrum of the annealed 200 nm CIS dandelions showed a threshold position at a longer wavelength region of ∼907 nm, which corresponded to a band gap of ∼1.36 eV for CIS nanostructures [8, 9]. The broad peak observed at around 540 nm in the absorption spectrum of annealed CIS dandelions was considered to possibly originate from the non-bonding copper localized states [39].

The N_2 adsorption–desorption isotherm of the as-prepared CIS dandelion is shown in figure 6(a). The BET specific surface area was calculated to be 44.5 $m^2\ g^{-1}$ based on the N_2 isotherms at 77 K. For comparison, we also prepared CIS nanoparticles by using the reported solvothermal process [8, 9]. The corresponding specific surface area, calculated from the N2 adsorption–desorption isotherm (see figure 6(b)), was only 8.2 $m^2\ g^{-1}$, which is more than five times smaller than that of the CIS dandelion structures.

To study the photoresponse characteristics, we measured the photocurrent of the photoswitching device fabricated by depositing 200 nm CIS dandelions onto reduced graphene oxide (rGO) electrodes followed by annealing at 350 ◦C under Ar atmosphere for 30 min, as described in section 2. The on–off cycles (see figure 7) under illumination confirmed the repeated production of photocurrent from the CIS dandelion structures. Here it is worth noting that there was no photocurrent obtained for pure rGO films under the same testing conditions. The fast photoresponsive behavior suggested that the CIS dandelion structures were highly light sensitive. The on–off performance of the device should be further optimized if the contact between the porous dandelion structures and the rGO electrode in the photoswitching device is improved.

4. CONCLUSION

In summary, we showed the synthesis of CIS nanodandelions by a two-step solvothermal approach. InSe dandelions were prepared in the first-step reaction and they then acted as structural templates and reacted with $Cu(acac)_2$ to induce the growth of CIS dandelions. The size of the dandelions could be controlled in the range from 200 nm to 2 μm by adjusting the amount of oleic acid added during the synthesis. The optical

absorption of the CIS dandelions showed the threshold at ~907 nm, which corresponded to a band gap energy of 1.36 eV. The BET measurements showed that the specific surface area of these CIS dandelion structures was 44.80 $m^2 g^{-1}$, which was more than five times larger than that of CIS quantum dots (e.g. 8.22 $m^2 g^{-1}$) prepared by using reported protocols. A fast photoresponsive behavior was demonstrated in a photoswitching device prepared using the 200 nm CIS dandelions as the active materials, which suggested their possible applications in optoelectronic devices.

5. ACKNOWELEDEGMENTS

The authors gratefully acknowledge AcRF Tier 1 RG 31/08 of MOE (Singapore) and NRF2009EWT-CERP001-026 (Singapore), Singapore A* STAR SERC grand 1021700144 and the Singapore Ministry of Education (MOE2010-T2-1- 017). HZ is grateful for the support of AcRF Tier 2 (ARC 10/10, No. MOE2010-T2-1-060) from MOE in Singapore and the New Initiative Fund FY 2010 (M58120031) from NTU, Singapore.

6. REFERENCES

[1] Miller A, Mackinnon A and Weaire D 1982 *Solid State Phys.* 36 119–75
[2] Devaney W E, Chen W S, Stewart J M and Mickelsen R A 1990 IEEE *Trans. Electron Devices* 37 428–33
[3] Xiao H Z, Yang L C and Rockett A 1994 J. *Appl. Phys*. 76 1503–10
[4] Mickelsen R A, Chen W S, Stewart J M and Devaney W E 1984 *J. Electrochem. Soc. Extended Abstracts* vol 84–2 (Pennington, NJ: Electrochemical Society) p 433
[5] Chernyak L, Jakubowicz A and Cahen D 1995 *Adv. Mater*. 7 45–8
[6] Moller H J 1993 Semiconductors for Solar Cells (Boston, MA: Artech House)
[7] Ward J S, Ramanathan K, Hasoon F S, Coutts T J, Keane J, Contreras M A, Moriarty T and Noufi R 2002 *Prog. Photovol*. **10** 41–6
[8] Tang J, Hinds S, Kelley S O and Sargent E H 2008 *Chem. Mater*. **20** 6906–10
[9] Panthani M G, Akhavan V, Goodfellow B, Schmidtke J P, Dunn L, Dodabalapur A, Barbara P F and Korgel B A *2008 J. Am. Chem. Soc*. **130** 16770–7
[10] Guo Q, Kim S J, Kar M, Shafarman W N, Birkmire R W, Stach E A, Agrawal R and Hillhouse H W 2008 *Nano Lett*. **8** 2982–7
[11] Allen P M and Bawendi M G 2008 *J. Am. Chem. Soc.***130** 9240–1
[12] Jiang Y, Wu Y, Mo X, Yu W C, Xie Y and Qian Y T 2000 Inorg. Chem. **39** 2964–5
[13] Yang Y H and Chen Y T 2006 *J. Phys. Chem*. B **110** 17370–4
[14] Li B, Xie Y, Huang J X and Qian Y T 1999 *Adv. Mater*. **11** 1456–9
[15] Norako M E and Brutchey R L 2010 *Chem. Mater*. **22** 1613–5
[16] Wang J J, Wang Y Q, Cao F F, Guo Y G and Wan L J 2010 *J. Am. Chem. Soc.* **132** 12218–21
[17] Zhu J X, Li A D and Yan Q Y 2010 *J. Nanosci. Nanotechnol*. **10** 7519–21
[18] Xu J, Lee C S, Tang Y B, Chen X, Chen Z H, Zhang W J, Lee S T, Zhang W X and Yang Z H 2010 ACS *Nano* **4** 1845–50
[19] Peng H L, Schoen D T, Meister S, Zhang X F and Cui Y 2007 *J. Am. Chem. Soc.* **129** 34–5
[20] Schoen D T, Peng H L and Cui Y 2009 *J. Am. Chem. Soc.***131** 7973–5
[21] Liu B and Zeng H C 2004 J. Am. Chem. Soc. 126 8124–5
[22] Cui Y and Lieber C M 2001 Science **291** 851–3
[23] Mann S and Ozin G A 1996 Nature **382** 313–8
[24] Wu H K, Thalladi V R, Whitesides S and Whitesides G M 2002 J. Am. Chem. Soc. 124 14495–502
[25] Lu Q Y, Gao F and Komarneni S 2004 *J. Am. Chem. Soc.* **126** 54–5
[26] Liu B and Zeng H C 2004 *J. Am. Chem. Soc.* **126** 16744–6 Qi X Y et al 2010 Adv. Funct. Mater. **20** 43
[27] Cao M H, He X Y, Chen J and Hu C W 2007 *Cryst. Growth Des*. **7** 170–4
[28] Purkayastha A, Yan Q Y, Raghuveer M S, Gandhi D D, Li H F, Liu Z W, Ramanujan R V, Borca-Tasciuc T and Ramanath G 2008 *Adv. Mater*. **20** 2679–83
[29] Yan Q Y, Raghuveer M S, Li H F, Singh B, Kim T, Shima M, Bose A and Ramanath G 2007 *Adv. Mater*. **19** 4358–63
[30] Xiao J, Yang H, Yin Z, Guo J, Boey F, Zhang H and Zhang Q 2011 *J. Mater. Chem.* **21** 1423–7

[31] Yin Z Y, Wu S X, Zhou X Z, Huang X, Zhang Q C, Boey F and Zhang H 2010 *Small* **6** 307–12
[32] Yan Q, Cheng H, Zhou W, Hng H H, Boey F Y C and Ma J 2008 *Chem. Mater*. **20** 6298–300
[33] Mokari T L, Zhang M J and Yang P D 2007 *J. Am. Chem. Soc.* **129** 9864–5
[34] Murphy J E, Beard M C, Norman A G, Ahrenkiel S P, Johnson J C, Yu P R, Micic O I, Ellingson R J and Nozik A J 2006 J. Am. Chem. Soc. 128 3241–7
[35] Zhu J X, Sun T, Hng H H, Ma J, Boey F Y C, Lou X W, Zhang H, Xue C, Chen H Y and Yan Q Y 2009 *Chem*. Mater. 21 3848–52
[36] Zhou W W, Zhu J X, Li D, Hng H H, Boey F Y C, Ma J, Zhang H and Yan Q Y 2009 Adv. Mater. **21** 3196–200
[37] Sánchez-Royoa J F, Seguraa A, Pellicer-Porresa J and Chevy A 2006 Surf. Sci. 600 3734–8
[38] Pathan H M, Kulkarni S S, Mane R S and Lokhande C D 2005 *Mater. Chem. Phys*. **93** 16–20
[39] Xiao J P, Xie Y, Xiong Y J, Tang Rand Qian Y T 2001 *J. Mater. Chem*. **11** 1417–20

List of Figures

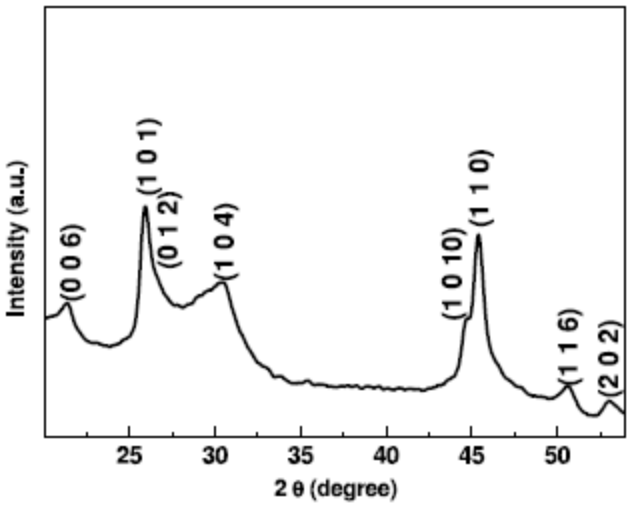
Intensity (a.u.)
(0 0 6)
(1 0 1)
(0 1 2)
(1 0 4)
(1 0 10)
(1 1 0)
(1 1 6)
(2 0 2)
25
30
35
40
45
50
2 θ (degree)

Figure 1

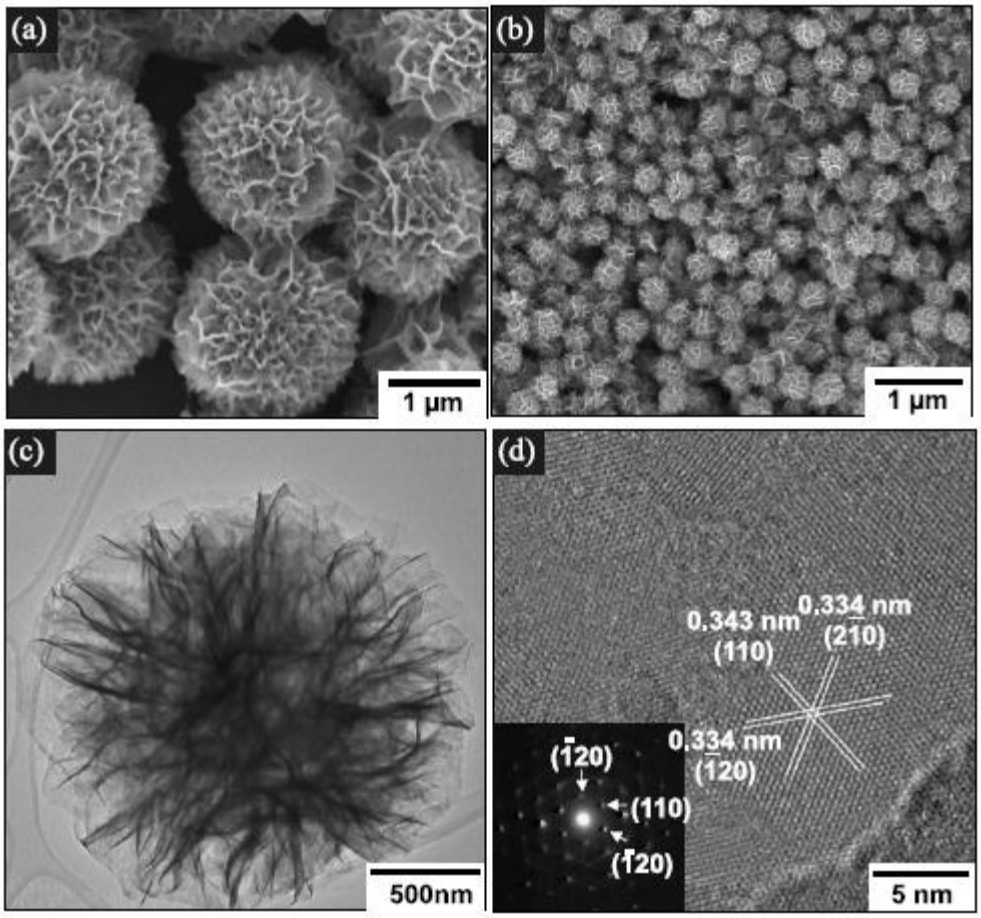
(a)
1 μm
(b)
1 μm
(c)
500nm
(d)
0.343 nm
(110)
0.334 nm
(2$\bar{1}$0)
0.334 nm
(1$\bar{2}$0)
($\bar{1}$20)
(110)
($\bar{1}$20)
5 nm

Figure 2

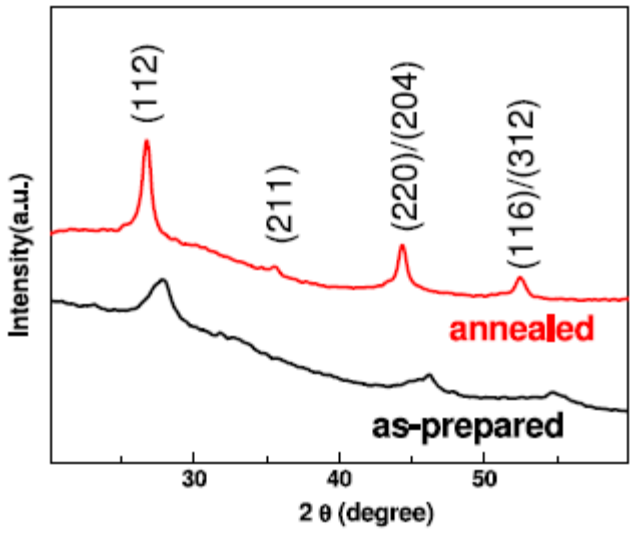
(112)
(211)
(220)/(204)
(116)/(312)
annealed
as-prepared
Intensity(a.u.)
30
40
50
2 θ (degree)

Figure 3

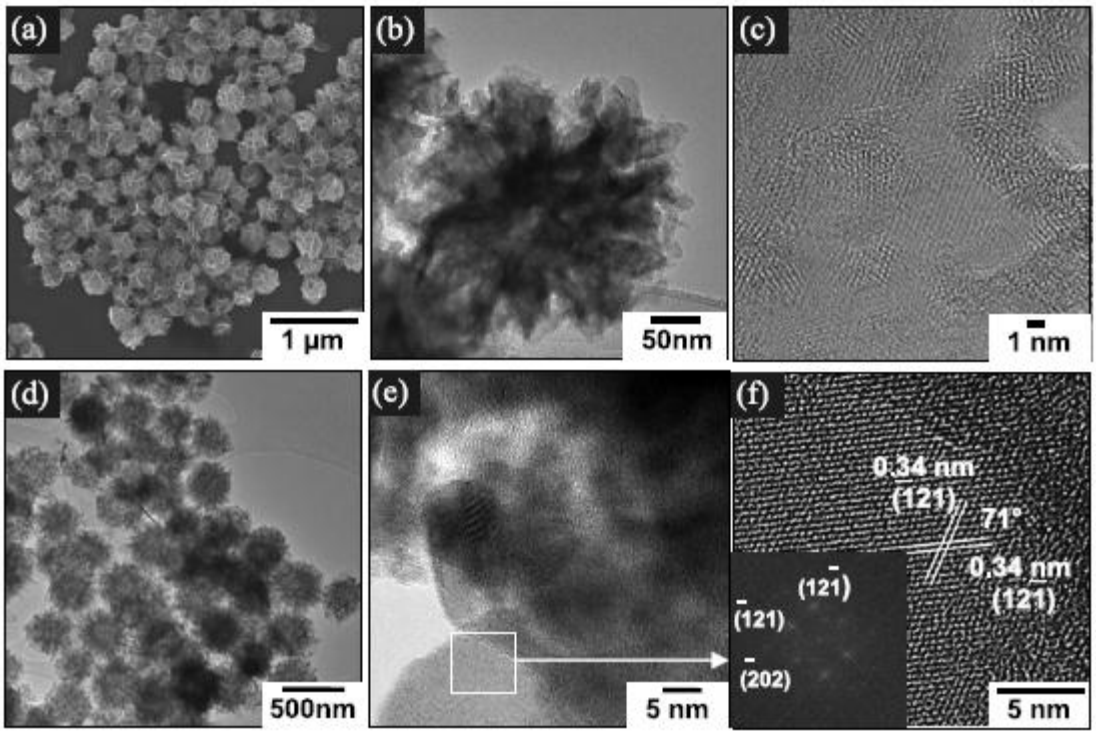
(a)
1 μm
(b)
50nm
(c)
1 nm
(d)
500nm
(e)
5 nm
(f)
0.34 nm
(121)
71°
0.34 nm
(121)
(121)
(121)
(202)
5 nm

Figure 4

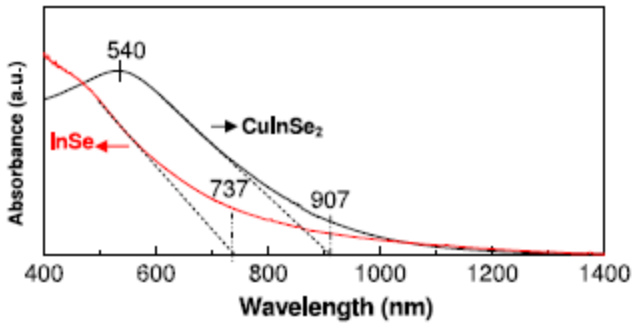
540
CuInSe2
InSe
737
907
Absorbance (a.u.)
400
600
800
1000
1200
1400
Wavelength (nm)

Figure 5

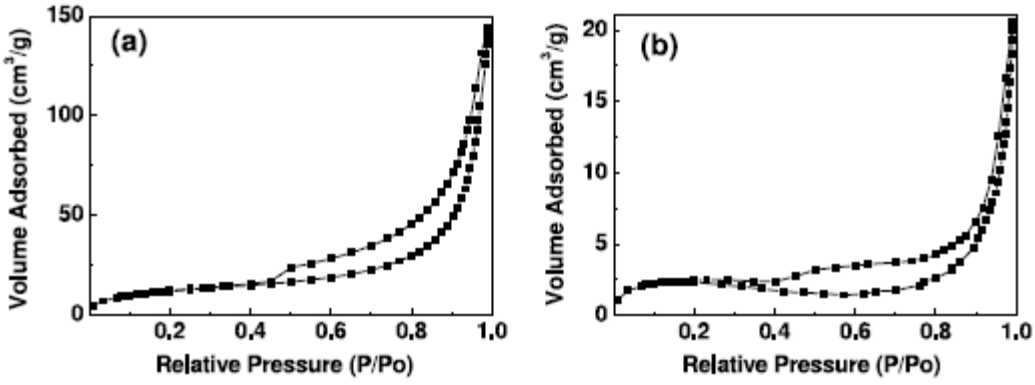
(a)
Volume Adsorbed (cm³/g)
150
100
50
0
0.2
0.4
0.6
0.8
1.0
Relative Pressure (P/Po)
(b)
Volume Adsorbed (cm³/g)
20
15
10
5
0
0.2
0.4
0.6
0.8
1.0
Relative Pressure (P/Po)

Figure 6

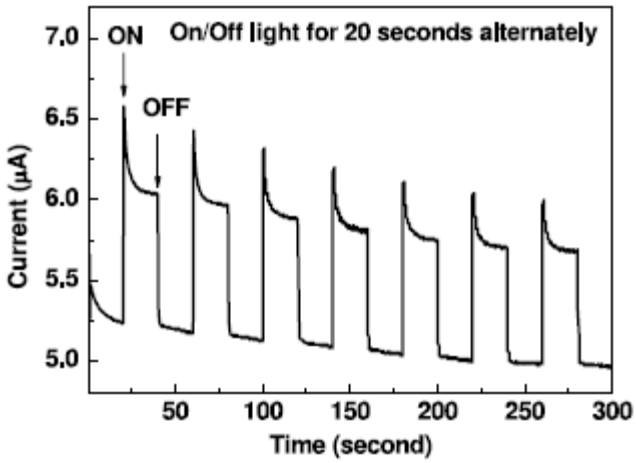
ON
On/Off light for 20 seconds alternately
OFF
Current (μA)
7.0
6.5
6.0
5.5
5.0
50
100
150
200
250
300
Time (second)

Figure 7